ELECTRON-ION RECOMBINATION, PHOTOIONIZATION AND DIELECTRONIC SATELLITE LINES OF Ca XVIII AND Ca XIX USING UNIFIED METHOD

Sultana N. Nahar
The Ohio State University

"APS - DAMOP 2007"
Calgary, Canada
June 5-10, 2007

Photoionization and Electron-Ion Recombination

$$\mathbf{Ca\ XVIII + h\nu \rightleftharpoons Ca\ XIX + \ \epsilon}$$

$$\mathbf{Ca\ XIX + h\nu \rightleftharpoons Ca\ XX + \ \epsilon}$$

- **These bound-free processes are inverse to each other**
- **Give rise to dielectronic satellite lines (DES)**

These may proceed as:

i) Photoionization (PI) & Radiative Recombination (RR)

$$\mathbf{X^{+Z} + h\nu \rightleftharpoons X^{+Z+1} + \epsilon}$$

ii) Autoionization (AI) & Dielectronic Recombination (DR)

$$\mathbf{e + X^{+Z} \rightleftharpoons (X^{+Z-1})^{**}} \rightleftharpoons \begin{cases} e + X^{+Z} & \text{AI} \\ X^{+Z-1} + h\nu & \text{DR} \end{cases}$$

- *Doubly excited autoionizing state [$(X^{+Z-1})^{**}$] introduces resonances*
- **RR and DR are inseparable in nature**

Theory: "UNIFIED METHOD" - (i) includes RR and DR, (ii) providex total electron-ion recombination rates self-consistent to photoionization cross sections, (iii) dielectronic satellite (DES) line strengths and profiles (*new extension*)

- **Calculational framework - close coupling approximation and R-matrix method (Nahar & Pradhan, PRL 1992, PRA 1994, PRA 2006)**

DIELECTRONIC SATELLITE (DES) LINES

- **DES lines - common in (e+He-like ion) collision spectra forming 3-electron Li-like ion and are used as diagnostics**

- **DES lines - form below the excitation threshold of the core. Ex. KLL (1s2l2l') satellite lines are below the core excitation $1s^2(^1S_0) \rightarrow 1s2p(^1P_1^o)$ of w-line**

- **DES lines - produced by radiation damping of doubly excited autoionizing states in dielectronic recombination.**

Ex. KLL (1s2l2l') complex introduces 22 DES lines (denoted as a,b,...,v - Gabriel 1972) as autoionizing states 1s2l2l' (1s2p2p, $1s2s^2$, $1s2p^2$) $\rightarrow$ $1s^22s(^2S_{1/2})$, $1s^22p(^2P^o_{1/2,3/2})$ bound states

Theoretical Treatment of DES lines

The earlier treatments

Based on isolated resonance approximation (initiated by Gabriel 1972) where the recombination rate coefficient (Bates & Dalgarno 1962) is given by

$$\alpha_R = a_o^3 \frac{g_i}{2g_f}\left[\frac{4\pi}{T}\right] e^{-\frac{\epsilon}{kT}} \frac{A_r A_a}{\Sigma_m A_a(m) + \Sigma_n A_r(n)} \tag{1}$$

ϵ is the DES energy

- Satellite lines are obtained at single energy points, ϵ.

The present treatment

Employs detailed photoionization cross sections for recombination cross sections

$$\sigma_{RC} = \sigma_{PI} \frac{g_i}{g_j} \frac{h^2\omega^2}{4\pi^2 m^2 c^2 v^2}.$$

where σ_{PI} includes autoionizing resonances

- Obtains intensity $I_s = \alpha_s \frac{n_i}{n_e}$, or intensity ratio $\frac{I_s}{I_w} = \frac{\alpha_s}{q_w}$, and resonant line strength $S = \int_{\epsilon_i}^{\epsilon_f} \sigma_{RC} d\epsilon$ from the unified σ_{RC} that includes both RR background and DR

- Provides energy profile of the satellite lines instead of a single point line

- Generates entire DES spectrum naturally

THEORY: Close-coupling (CC) R-matrix method

Total wavefunction expansion in CC approximation:

$$\mathbf{\Psi_E(e+ion) = A\sum_{i}^{N}\chi_i(ion)\theta_i + \sum_{j} c_j\Phi_j(e+ion)}$$

χ_i → **target/core ion wavefunction,**
Φ_j → **correlation functions of (e+ion) system**
θ_i → **electron (bound or continuum) wavefunction**
• **The complex resonant structures in collisional and radiative processes are included through channel couplings.**

The Iron Project - The relativistic Hamiltonian in Breit-Pauli R-matrix (BPRM) approximation:

$$\mathbf{H^{BP}_{N+1} = H^{NR}_{N+1} + H^{mass}_{N+1} + H^{Dar}_{N+1} + H^{so}_{N+1},}$$

where the non-relativisitc Hamiltonian is

$$\mathbf{H^{NR}_{N+1} = \sum_{i=1}^{N+1}\left\{-\nabla_i^2 - \frac{2Z}{r_i} + \sum_{j>i}^{N+1}\frac{2}{r_{ij}}\right\}.}$$

Mass correction term → $\mathbf{H^{mass}_{N+1}} = -\frac{\alpha^2}{4}\Sigma_i\, \mathbf{p_i^4}$, **Darwin term** → $\mathbf{H^{Dar}_{N+1}} = \frac{Z\alpha^2}{4}\Sigma_i\, \nabla^2(\frac{1}{r_i})$, **Spin-orbit interaction term** → $H^{so}_{N+1} = Z\alpha^2\,\Sigma_i\,\frac{1}{r_i^3}\mathbf{l_i.s_i}$

Sovle Schordinger equation: $\mathbf{H^{BP}_{N+1}}\Psi_E(e+ion) = E\Psi_E(e+ion)$

The channels introduce a set of coupled equations which are solved by R-matrix method

• $\mathbf{E < 0}$ → **Bound (e+ion) states** Ψ_B
• $\mathbf{E \geq 0}$ → **Continuum states** Ψ_F

Photoionization/Recombination Transition Matrix elements: $< \Psi_B || \mathbf{D} || \Psi_F >$

D= $\Sigma_n r_n \rightarrow$ **dipole operator** n **= number of electrons**

The generalized line strength (S)

$$\mathbf{S} = | < \mathbf{\Psi_j} || \mathbf{D} || \mathbf{\Psi_i} > |^2 = \left| \left\langle \Psi_\mathbf{f} | \sum_{\mathbf{j=1}}^{\mathbf{N+1}} \mathbf{r_j} | \Psi_\mathbf{i} \right\rangle \right|^2 ,$$

The photoionization cross section is

$$\sigma_{\mathbf{PI}} = \frac{\mathbf{4}\pi}{\mathbf{3c}} \frac{\mathbf{1}}{\mathbf{g_i}} \omega \mathbf{S},$$

Recombination cross section, $\sigma_{\mathbf{RC}}$**, is related to** $\sigma_{\mathbf{PI}}$ **as,**

$$\sigma_{\mathbf{RC}} = \sigma_{\mathbf{PI}} \frac{\mathbf{g_i}}{\mathbf{g_j}} \frac{\mathbf{h^2} \omega^2}{\mathbf{4} \pi^2 \mathbf{m^2 c^2 v^2}}.$$

The recombination rate coefficient, $\alpha_{\mathbf{RC}}$**, is obtained as**

$$\alpha_{\mathbf{RC}}(\mathbf{T}) = \int_0^\infty \mathbf{v f(v)} \sigma_{\mathbf{RC}} \mathbf{dv},$$

$f(v)$ **= Maxwellian velocity distribution function**

Total α_{RC} $\rightarrow$ **Contributions from infinite number of recombined states**

Dielectronic Satellites (DES) from the Unified Method

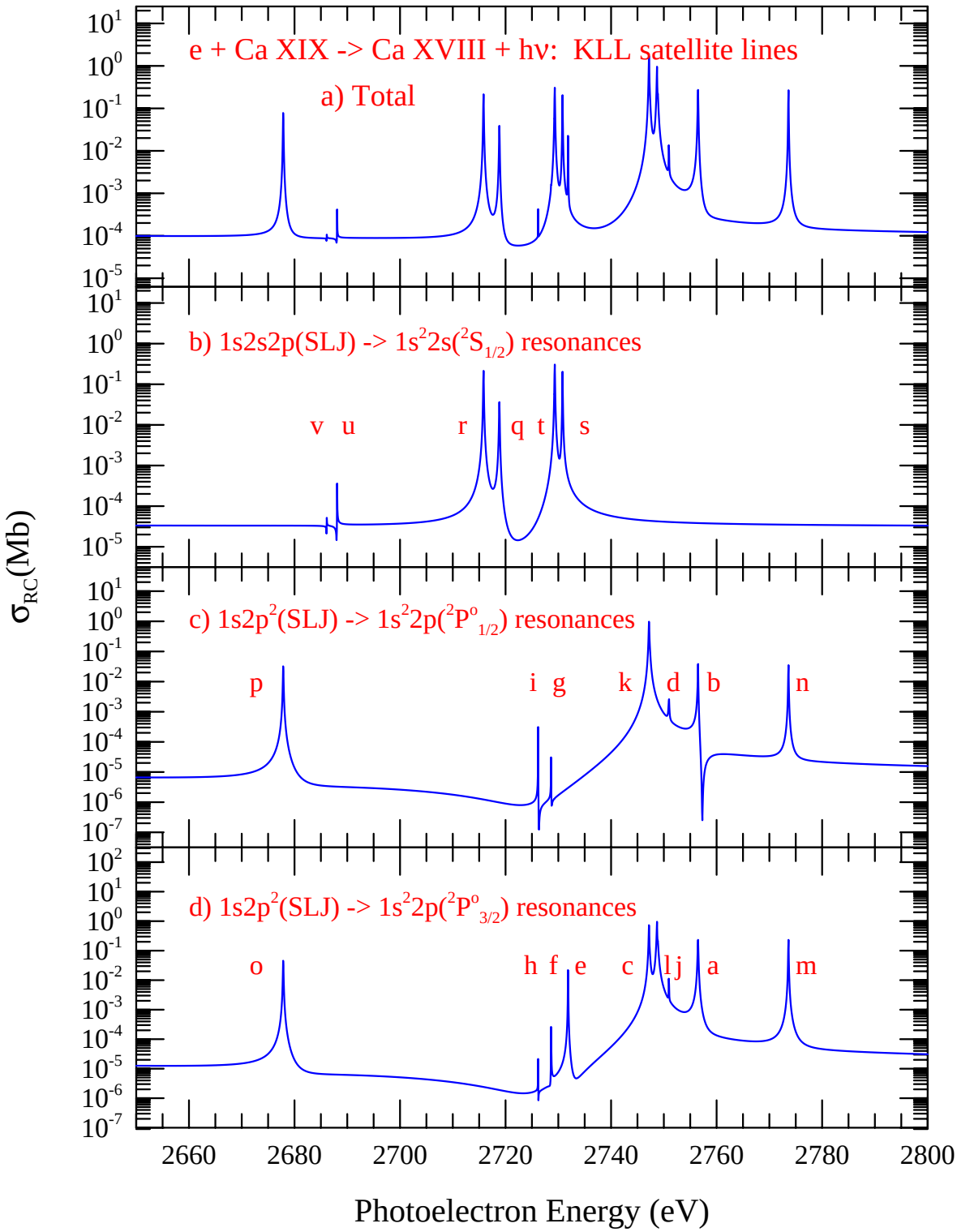

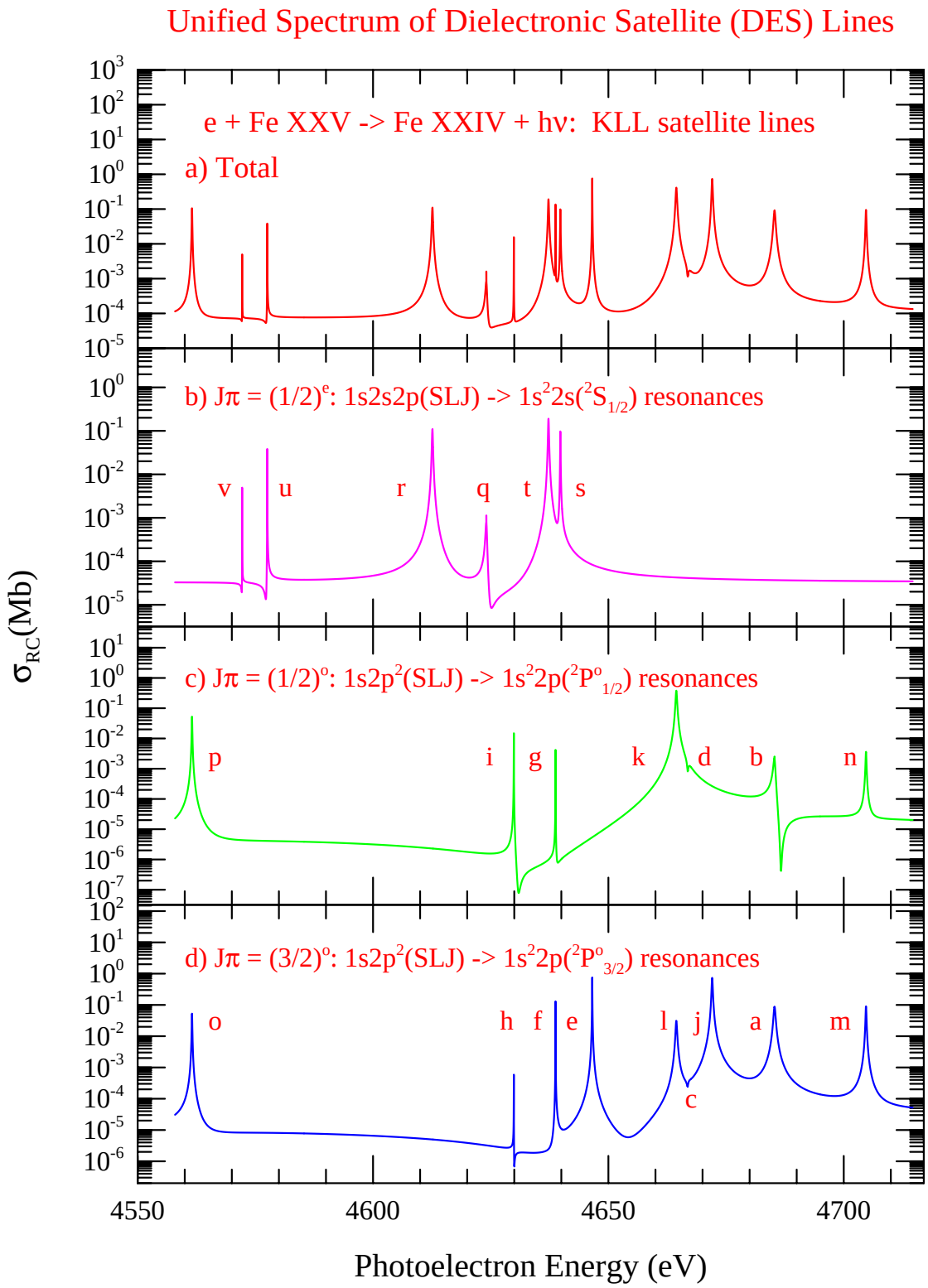
Unified Spectrum of Dielectronic Satellite (DES) Lines
e + Fe XXV -> Fe XXIV + hν: KLL satellite lines
a) Total
b) Jπ = (1/2)e: 1s2s2p(SLJ) -> 1s22s(2S1/2) resonances
v u r q t s
c) Jπ = (1/2)o: 1s2p2(SLJ) -> 1s22p(2Po1/2) resonances
p i g k d b n
d) Jπ = (3/2)o: 1s2p2(SLJ) -> 1s22p(2Po3/2) resonances
o h f e l j a m c
σRC(Mb)
4550
4600
4650
4700
Photoelectron Energy (eV)

Comparison - DES Intensity ratios $I(KLL)/I(w)$ - Fe XXV (Nahar, Oelgoetz, Pradhan 2007)

solid line – present, dashed line – Bely-Dubau et al. (1982), dotted line – Vainshtein and Safronova (1978)

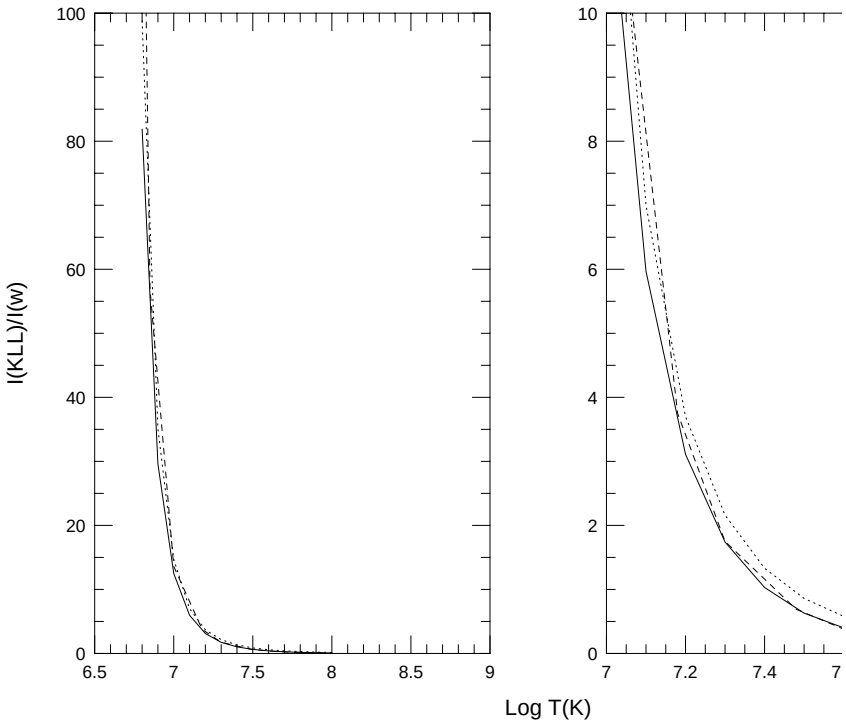

- **Present unified DES line strengths are in good agreement with those in the individual resonance approximation, BUT some significant differences are found in temperature ranges around Log T(K) = 7.2 where the DES lines are most temperature sensitive, below the temperature of maximum abundance at Log T(K) = 7.4 for Fe XXV in coronal equilibrium.**

Comparison of DES spectra of He-like Fe XXV at T = 1.47 $\times 10^7$ K using the relativistic distorted wave (RDW) data from the Los Alamos codes (black) and the present DES strengths computed using the unified recombination scheme (green) (Nahar, Oelgoetz, Pradhan 2007)

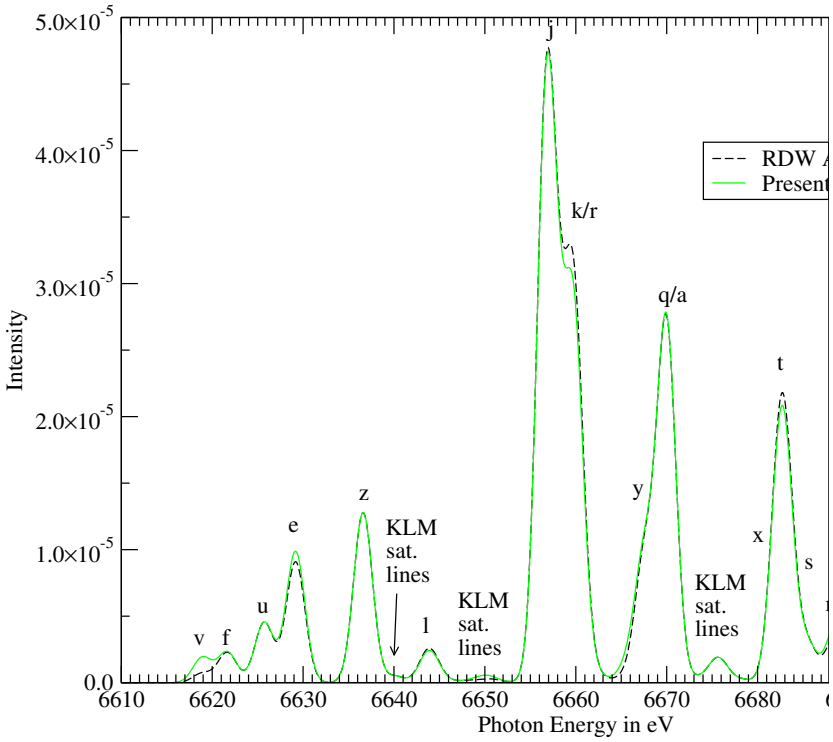

- **The first application for Fe XXV spectrum shows excellent agreement with that from Los Alamos data.**

Table: The energies (eV) and strengths of DES lines in KLL resonance complex of (e + Ca XIX) from the unified method.

Key	Transition	E(eV)	Peak
o	$1s2s^2(^2S_{1/2}) \rightarrow 1s^22p(^2P^o_{3/2})$	2678	4.567E-02
p	$1s2s^2(^2S_{1/2}) \rightarrow 1s^22p(^2P^o_{1/2})$	2678	3.225E-02
v	$1s2p^3P^o2s(^4P^o_{1/2}) \rightarrow 1s^22s(^2S_{1/2})$	2686	5.171E-05
u	$1s2p^3P^o2s(^4P^o_{3/2}) \rightarrow 1s^22s(^2S_{1/2})$	2688	3.614E-04
r	$1s2p^1P^o2s(^2P^o_{1/2}) \rightarrow 1s^22s(^2S_{1/2})$	2716	2.143E-01
q	$1s2p^1P^o2s(^2P^o_{3/2}) \rightarrow 1s^22s(^2S_{1/2})$	2719	3.635E-02
i	$1s2p^2(^4P_{1/2}) \rightarrow 1s^22p(^2P^o_{1/2})$	2726.4	3.110E-04
h	$1s2p^2(^4P_{1/2}) \rightarrow 1s^22p(^2P^o_{3/2})$	2726	2.134E-05
t	$1s2p^3P^o2s(^2P^o_{1/2}) \rightarrow 1s^22s(^2S_{1/2})$	2729	3.060E-01
f	$1s2p^2(^4P_{3/2}) \rightarrow 1s^22p(^2P^o_{3/2})$	2729	2.616E-04
g	$1s2p^2(^4P_{3/2}) \rightarrow 1s^22p(^2P^o_{1/2})$	2729	3.079E-05
s	$1s2p^3P^o2s(^2P^o_{3/2}) \rightarrow 1s^22s(^2S_{1/2})$	2731	2.033E-01
e	$1s2p^2(^4P_{5/2}) \rightarrow 1s^22p(^2P^o_{3/2})$	2732	2.204E-02
k	$1s2p^2(^2D_{3/2}) \rightarrow 1s^22p(^2P^o_{1/2})$	2747	9.738E-01
l	$1s2p^2(^2D_{3/2}) \rightarrow 1s^22p(^2P^o_{3/2})$	2749	9.559E-01
d	$1s2p^2(^2P_{1/2}) \rightarrow 1s^22p(^2P^o_{1/2})$	2751	2.612E-03
c	$1s2p^2(^2P_{1/2}) \rightarrow 1s^22p(^2P^o_{3/2})$	2747	7.312E-01
j	$1s2p^2(^2D_{5/2}) \rightarrow 1s^22p(^2P^o_{3/2})$	2749	2.192E-01
b	$1s2p^2(^2P_{3/2}) \rightarrow 1s^22p(^2P^o_{1/2})$	2756	3.835E-02
a	$1s2p^2(^2P_{3/2}) \rightarrow 1s^22p(^2P^o_{3/2})$	2756	2.323E-01
m	$1s2p^2(^2S_{1/2}) \rightarrow 1s^22p(^2P^o_{3/2})$	2774	2.320E-01
n	$1s2p^2(^2S_{1/2}) \rightarrow 1s^22p(^2P^o_{1/2})$	2774	3.519E-02

X-Ray Modeling of Solar Corona and Flares: "Halloween" Solar Storm (Oct 28, 2003)

active region with big sunspot erupts ….

8 minutes later ... X-class Flare observed on the Earth

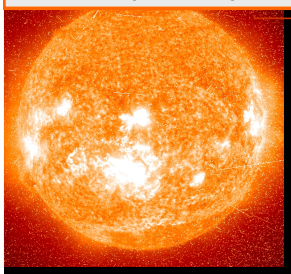

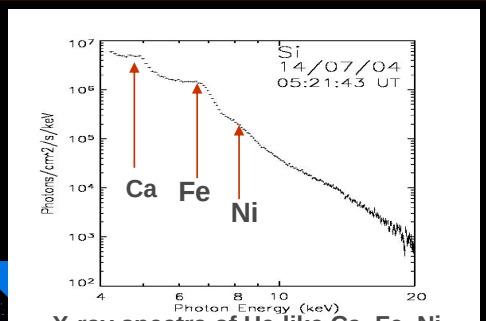

X-ray spectra of He-like Ca, Fe, Ni (SOXS Mission, PRL, India)

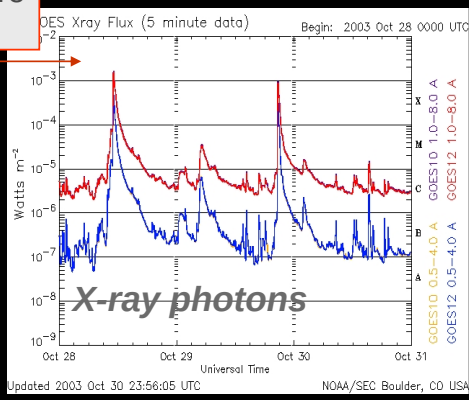

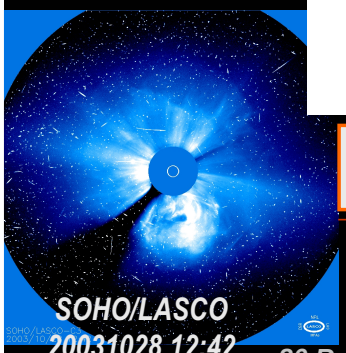

SOHO/LASCO
20031028 12:42

coronal mass ejection leaves the Sun ….

8 hours later... particles saturate SOHO/LASCO detector and reach the Earth ("proton shower")

30 R_{sun}

heliosphere

… at L1 20031028 20:49

NOAA National Weather Service

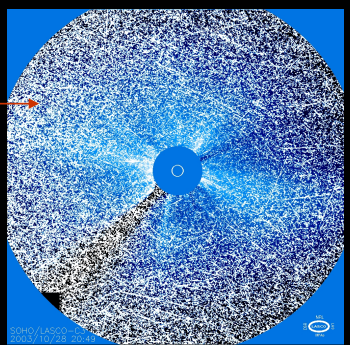

CONCLUSION

1. **We present results from ab initio unified method for photoionization and recombination of Ca XVIII, Ca XIX**
2. **Results includes total and level specific recombination rates and photoionization cross sections of hundreds of bound levels.**
3. **Total recombination rate coefficients show higher rates at high T compared to previous theoretical results**
4. **Self-consistent sets of atomic data for photoionization, recombination are obtained and should yield more accurate astrophysical photoionization models**